



## The dysraphic levels of skin and vertebrae are different in mouse fetuses and neonates with myelomeningocele

Dorothea Stiefel<sup>a,b,\*</sup>, Martin Meuli<sup>a</sup>

<sup>a</sup>Department of Pediatric Surgery, University Children's Hospital Zürich, 8032 Zürich, Switzerland

<sup>b</sup>Institute of Child Health, Neural Development Unit, University College London, London WC1N 1EH, UK

### Key words:

Spina bifida;  
Myelomeningocele;  
Dysraphism;  
Neural tube defect;  
Fetal surgery

### Abstract

**Background:** Mouse fetuses with spontaneous myelomeningocele (MMC) were investigated, determining the various levels of dysraphism in soft tissue, spinal cord, and vertebrae. Morphology was correlated with hind limb function.

**Methods:** Viable *curly tail/loop tail* mouse fetuses underwent qualitative standardized ex utero examination of tail and hind limb sensitivity and motor response. Afterward, they were processed either for histology or skeletal preparation.

**Results:** All animals displayed identical cranial levels of soft tissue and neural defects. The cranial opening of the vertebral defects were invariably located more cranially (range, 0.5-5 vertebrae; mean = 2.25). The caudal opening of soft/neural tissue and bony defects was invariably at the coccygeal base. The comparison of functional with morphological levels demonstrated that, in 52.5%, the level of the soft/neural tissue dysraphism and, in 47.5%, the level of the bony opening correlated with the neurologic deficit.

**Conclusion:** The naturally occurring soft tissue coverage over the MMC could exert a protective effect toward the underlying spinal cord. This interpretation supports the concept that in utero acquired destruction of exposed neural tissue is a main factor for the neonatal functional deficit. Thus, these data are consistent with the rationale for prenatal MMC repair in humans.

© 2008 Published by Elsevier Inc.

Myelomeningocele (MMC) is the most severe form within the relatively broad spectrum of neural tube defects and represents the morphological end result of failed neurulation during early embryonic life. The classic anatomical hallmarks in humans are a nonneurulated spinal cord resting on the dorsal aspect of a cystic cerebrospinal

fluid-filled sac, missing dorsal arches of the affected vertebrae, missing soft tissue, and skin over the lesion [1,2].

Unsystematic own observations from previous studies in a mouse model with genetically determined MMC indicated that the rostral opening of the involved neurocutaneous defect might be distinctly different from the bony defect of the same specimen.

Therefore, the present study was designed to formally address the question to what extent these presumed variations were factual, and if so, whether these differences could have a measurable impact on neurologic function.

\* Corresponding author. Department of Surgery, University Children's Hospital Zürich, 8032 Zürich, Switzerland. Fax: +41 44 266 71 71.

E-mail address: stiefel\_d@yahoo.co.uk (D. Stiefel).

## 1. Materials and methods

### 1.1. Breeding and collection of specimens

All animal experiments were performed in accordance with the regulations of the Animals (Scientific Procedures) Act 1986 of the UK Government. The well-established animal model of the *loop tail* (*Lp*) and *curly tail* (*ct*) mutant mouse strains was used. Doubly heterozygous *loop tail/curly tail* males (*Lp*<sup>+/+</sup>*ct*<sup>+/+</sup>) were mated overnight with homozygous *curly tail* females (*ct*<sup>+/+</sup>*ct*<sup>+/+</sup>), generating litters containing pups with straight tails (40.5%), with curly tails alone (25.5%), or with curly tails and spina bifida (SB) (34%). To collect neonates, we waited for pregnant females to litter, whereas for collecting fetuses, pregnant females were culled by cervical dislocation. Fetuses were dissected out of the uterus. A subset of animals was left on placental support and kept in Dulbecco's modified Eagle's medium (Gibco, BRL, Life Technologies, LTD, Paisley, UK) containing 10% fetal calf serum to assess them neurologically (see below). Thereafter, all fetuses were culled on a frozen metal plate and neonates by an overdose of midazolam/fentanyl (Hypnorm/Hypnovel). All animals were rinsed in phosphate-buffered saline and processed for skeletal preparation or histology as described below.

Animals with small and large SB were collected. MMC lesions were classified based on the ratio of total body size to MMC size (Table 1). The internal control group (CT) consisted of animals without SB, that is, with straight or curly tails in equal shares.

### 1.2. Neurologic assessment

A subset of SB and control fetuses and neonates was selected for qualitative neurologic assessment. Animals between gestational stages E16.5 and E18.5 and on neonatal day P1 were collected as described above ( $n = 47$ ; E16.5 SB/CT = 9/2, E17.5 SB/CT = 6/2, E18.5 SB/CT = 13/2, P1 SB/CT = 11/2; Table 2). Younger animals were not examined because a pilot test series revealed that no reaction was obtainable in hind limbs in both control and SB animals. This is probably because of physiologic immaturity of the nervous

system for all animals at these early stages [3-5]. According to Zeman et al [6], murine hind limbs are innervated by the spinal roots T12 through L3.

Performance of functional tests was limited to the first 4 minutes after culling the mother to guarantee vital reactions of the examined fetuses. Thus, usually, only one SB and one control animal could be examined from each litter.

The following qualitative functional tests, described in more detail elsewhere [5], aiming at eliciting a classic pain reaction were performed in a standardized way 3 times in each individual: pinching with microforceps on the midshaft of radius and ulna, tibia and fibula, and tail. Results were defined as conclusive if the response pattern obtained was identical in all 3 consecutive attempts. Thereafter, all specimens were processed for histology or skeletal preparation as described below.

### 1.3. Histology

Spina bifida and control animals were collected from embryonic day E16.5 to E18.5 and on neonatal day P1 ( $n = 20$ ; 4 SB and 1 control specimen for each stage, Fig. 1). They were fixed in Bouin's solution (Sigma, Poole, Dorset, UK) for 4 to 7 days. After serial dehydration, they were embedded in paraffin wax. Sagittal sections were cut with a rotary microtome (Microm HM330) at 12- $\mu$ m thickness. After dewaxing with Histo-Clear (National Diagnostics, London, UK), the slides were serially rehydrated to distilled water, stained with Ehrlich's hematoxylin (10 minutes) and eosin (5 minutes), finally dehydrated, mounted in DPX, and coverslipped.

### 1.4. Whole-body skeletal preparation

This preparation modality renders soft tissues transparent and colorless without damaging tissue integrity, thus, allowing direct visualization of the skeleton (cartilage stains blue, bone stains red).

Fetal animals between E15.5 and E18.5 and neonates on P1 were collected as described above ( $n = 94$ ; E15.5 SB/CT = 5/5, E16.5 SB/CT = 19/5, E17.5 SB/CT = 11/5, E18.5 SB/CT = 18/5, P1 SB/CT = 16/5; Table 3, Fig. 2). Before fixation in 4% paraformaldehyde/phosphate-buffered saline, animals were eviscerated and deskinning, leaving a small cutaneous rim around the MMC circumference to keep the lesion intact. The most proximal (cranial) end of the well-visible cutaneous opening of the SB lesion was marked with a microsurgical 10/0 suture to allow direct comparison of cutaneous and skeletal dysraphic levels in the same animal after skeletal preparation as follows: Specimens were placed in Alcian blue solution for 6 days at 4°C, rehydrated, transferred into alizarin red solution for 3 hours, and finally taken through a series of glycerol-potassium hydroxide solutions to clear the surrounding soft tissue. Storage followed in 100% glycerol at room temperature.

**Table 1** Classifying MMC size in SB animals

	Gestational age		Ratio*
	E16.5	E18.5	
Total body length (mm)**	15-18	26-28	
Large MMC length (mm)**	3-5	4-6	<10
Small MMC length (mm)**	1.5	2	>10

\* Ratio = total body length/MMC length.

\*\* Lengths shown are the ranges typically seen in the study.

**Table 2** Correlation of functional assessment with morphology (neurocutaneous and skeletal opening)

	Th 11	Th 12	L 1	L 2	L 3	L 4	L 5	L 6	S 1	S 2	S 3	S 4	S 5	S 6
P1; n=11					SSSSS	SSSSS	SSSSS	SSSSS						
E18.5; n=13			SSSSS	SSSSS	SSSSS	SSSSS	SSSSS	SSSSS						
				NNNN	NNNN	NNNN	NNNN	NNNN	NNNN	NNNN	NNNN	NNNN	NNNN	NNNN
E17.5; n=6					SSSSS	SSSSS	SSSSS	SSSSS						
					NNNN	NNNN	NNNN	NNNN	NNNN	NNNN	NNNN	NNNN	NNNN	NNNN
E16.5; n=9						SSSSS	SSSSS	SSSSS						
						NNNN	NNNN	NNNN	NNNN	NNNN	NNNN	NNNN	NNNN	NNNN

Each gray bar represents the distance between the rostral level of the skeletal opening of the MMC lesion (double line) and the rostral level of the cutaneous opening of the lesion (single line) within the same animal. The age ranges from the first postnatal day (P1) to embryonic stages at day 16 (E16.5). Light gray bars represent animals without any pain reaction in hind limbs nor tails. Dark gray bars indicate animals showing only pain reaction in hind limbs but none in tails. Note that physiologic innervation of murine hind limbs is effected by spinal nerve roots T12 through L3 [6]. Therefore, only animals with a rostral skeletal level above L3 and a rostral neurocutaneous level below L3 allow for correlation of morphology and function within the same animal (n = 21). These animals are marked with capital letters (S or N) within the bar. As a final result, 47.5% of the specimens show a functional level that coincides with the skeletal level (animals marked with S) and 52.5% with a function that corresponds with the neurocutaneous level (marked with N). T11/12 indicates thoracic levels; L1-6, lumbar levels; S1-6, sacral levels.

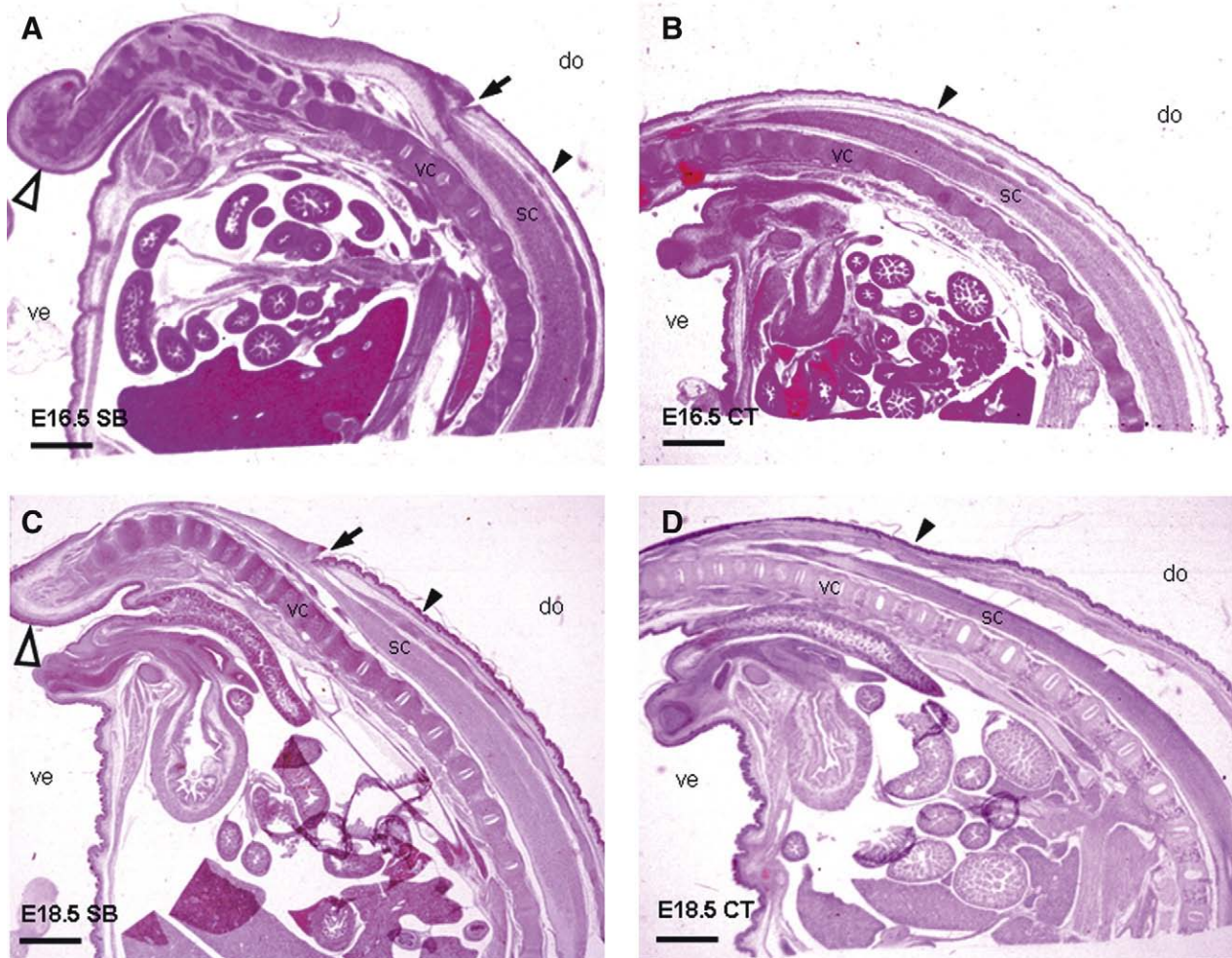


**Fig. 1** Hematoxylin-eosin-stained sagittal sections through the spinal cord of SB (A, C) and control (B, D) animals on E16.5 and E18.5, showing the lumbosacral end of the specimen. The closed arrowhead marks the epidermis, the arrow marks the cranial end of the MMC lesion. At this site, the coincidence of the epidermal with the neural opening of the SB lesion can easily be appreciated. do indicates dorsal; ve, ventral; vc, vertebral column; sc, spinal cord; arrow, cranial end of the SB; black closed arrowhead, skin; black open arrowhead, curly tail. Scale bars in micrometers: A, B = 1000; C, D = 1330.

## 1.5. Photographic documentation

Photographic documentation was obtained with color reversal films using a light microscope (Stemi SV 11, Zeiss, Welwyn Garden City, UK).

## 2. Results

### 2.1. Neurologic assessment

Control animals always demonstrated identical reactions to the stimuli applied. After pinching the paw of the upper or lower limb, the animals showed a withdrawal-like movement of the respective limb, squirming of the ipsilateral body side, and mouth opening (silent or audible shriek, depending on the age of the animal). Tail pinching consistently evoked a similar

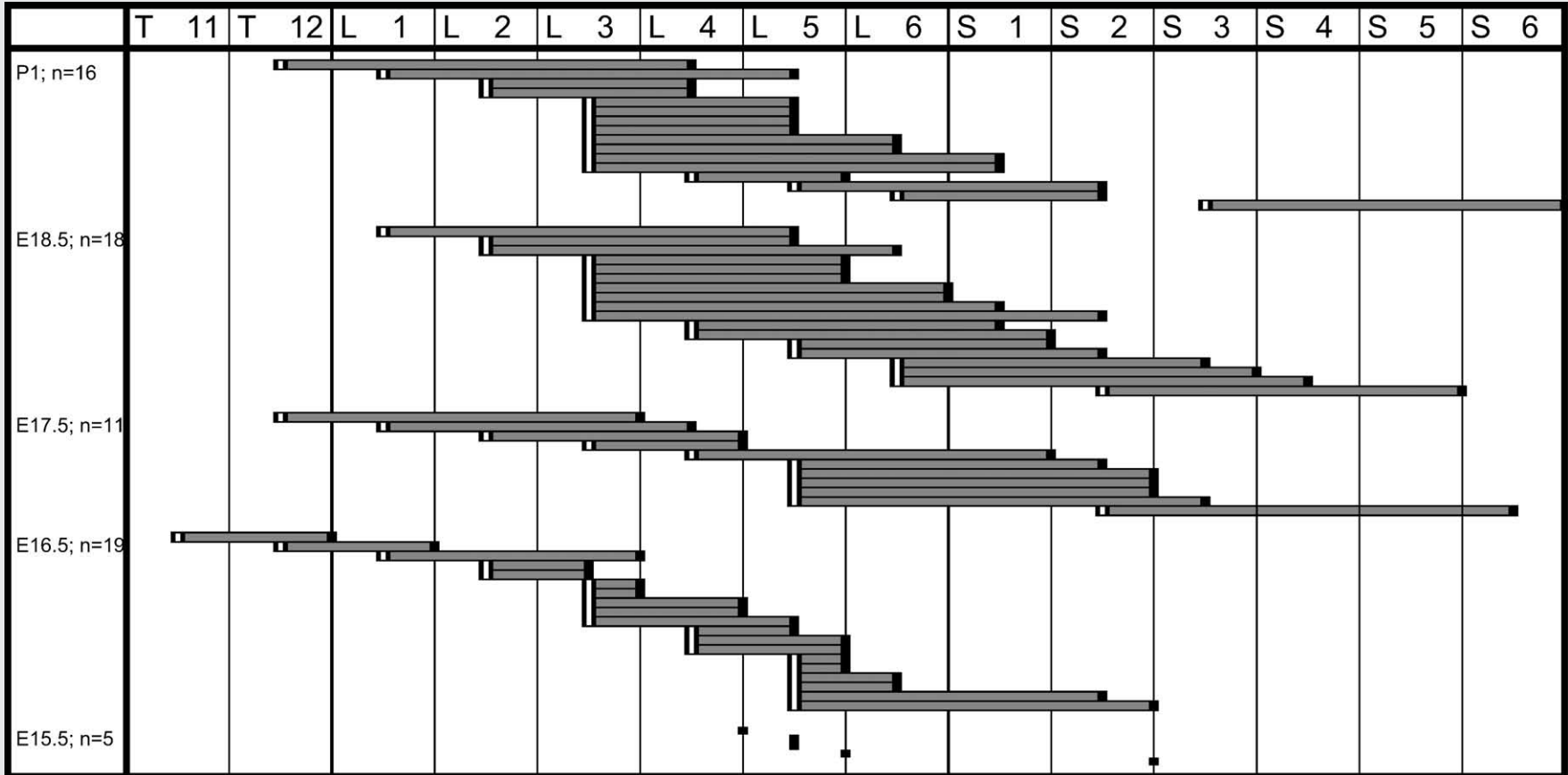
reaction, including squirming and mouth opening. These reaction patterns were interpreted as physiologic and, thus, defined as normal murine fetal or neonatal pain reactions.

The test results of SB animals are shown in detail in [Table 2](#). Briefly, the same, that is, normal pain reaction as described above was found in all animals at all stages after forelimb pinching. After tail pinching, none of the animals showed a pain reaction. When testing the hind limbs, a pain reaction was only found in animals with a small lesion (59%,  $n = 23$ ). Animals with large lesions exhibited no pain reaction in hind limbs or tail (41%,  $n = 16$ ).

### 2.2. Histology

To determine the cranial and caudal levels of the nonneurulated spinal cord and to correlate them with the corresponding levels of the skin opening, we made sagittal sections ([Fig. 1](#)). We found in all animals at all stages that the

**Table 3** Skeletal vs neurocutaneous opening of the rostral end of the SB lesion



Each gray bar represents the distance between the rostral level of the skeletal opening of the SB lesion (double line) and the rostral level of the cutaneous opening of the lesion (single line) within the same animal (n = 69). The age ranges from the first postnatal day (P1) to embryonic stage at day 15 (E15.5). Note that the skeletal opening is always located rostrally to the neurocutaneous opening with a difference ranging from 0.5 to 5 vertebrae (mean = 2.25). At E15.5, the skeletal opening (double line) is not presented because physiologic arch fusion of the vertebral column has not taken place and is only accomplished by E16.5. Thus, only the neurocutaneous opening (single line) can be determined at this early stage. The overall results show clearly that the rostral levels of the neurocutaneous and skeletal opening vary considerably between individuals, also within the same stage. T11/12 indicates thoracic levels; L1-6, lumbar levels; S1-6, sacral levels.

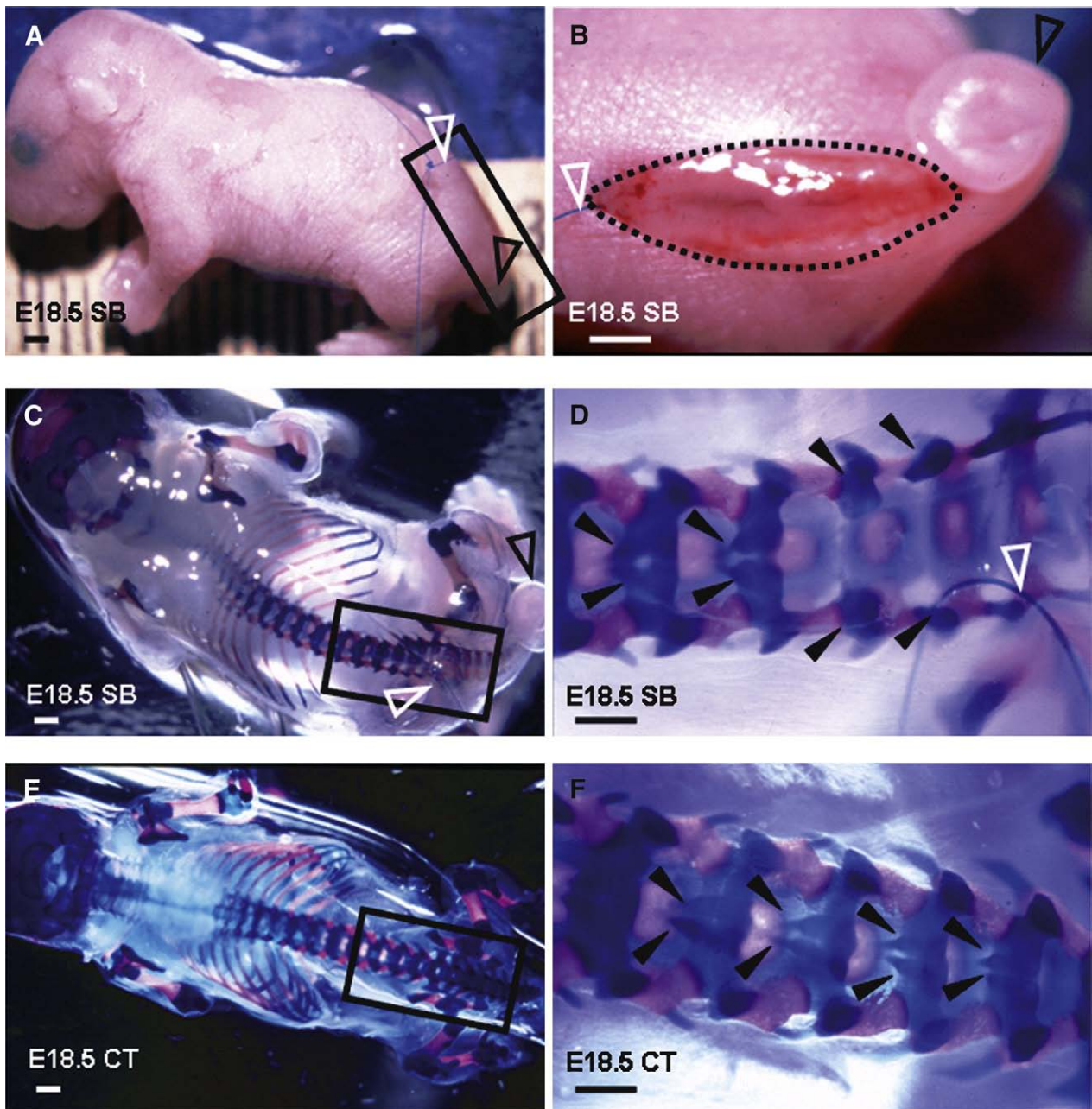


**Fig. 2** E18.5 animals before (A, B) and after (C-F) skeletal preparation. Panels A to D stem from the same SB lesion and E to F from the same control (CT) animal. Panels B, D, and F show the respective magnifications from the areas delineated by rectangles in panels A, C, and E. The dotted line in panel B outlines the SB lesion. The white open arrowheads show the suture marking the cranial end of the lesion. The black open arrowheads point at the curled tail. Closed arrowheads mark the vertebral arches, either fused in control animals (F) and partly fused/partially unfused in SB animals (D). Note the difference (in this example, 2 vertebral bodies) between the cutaneous level of the MMC marked with a suture (white open arrowhead) and the skeletal level of the dysraphic vertebrae (closed arrowhead, D). In all illustrations (A to F), left = cranial, right = caudal; panel A is a side view; panels B and C to F are top views. White open arrowhead indicates suture; black open arrowhead, curly tail; black closed arrowhead, (un)fused dorsal arches; blue stained tissue, cartilage; red stained tissue, osseous tissue. Scale bars in micrometers: A to F = 1000.

cranial as well as the caudal end of the neural placode coincided with the skin opening. However, interindividual comparison revealed that all lesions were of variable size, extending invariably from the base of the consistently curled tail (base of coccyx) to a variable level of the thoracic, lumbar, or sacral spine.

### 2.3. Whole-body preparation

This investigation was made to allow identification and correlation of skin and skeletal dysraphic levels in the same animal. Detailed results are compiled in Table 3; an illustrative specimen is shown in Fig. 2.

We found at E15.5 that all specimens showed unfused dorsal arches. Thus, distinction between control and SB animals after skeletal preparation was only possible because of the suture marking in the cranial end of the SB lesion. By E16.5, physiologic fusion of the vertebral dorsal arches was completed in control animals (Fig. 2E, F). Therefore, E16.5, SB specimens presented unfused vertebral arches (Fig. 2D) at the site of the MMC lesion starting on variable cranial levels and always extending down to the coccyx; that is, the skeletal defect showed a similar pattern of distribution as the corresponding neurocutaneous lesion seen in histologic sections. Correlation of the cranial end of the skeletal defect with the suture-marked cranial end of the skin defect (Fig. 2A-D) demonstrated in the same animal that dysraphism of the vertebrae was always located more cranially than dysraphism of the neurocutaneous defect. The difference ranged from 0.5 to 5 vertebrae (mean = 2.25; Table 3, Fig. 2D).

In summary, although the skeletal and neurocutaneous lesions varied significantly in size inter- and intraindividually, we consistently found that the neurocutaneous opening at its cranial end was always located more caudally than the cranial end of the bony dysraphism, whereas at the caudal end of the lesion, both the neurocutaneous and the vertebral dysraphism coincided invariably.

#### 2.4. Correlation of functional and dysraphic levels

The data correlating functional and morphological, that is, neurocutaneous and skeletal levels of each animal are shown in Table 2. Essentially, in 46% (n = 18) of all functionally tested animals, skeletal and neurocutaneous levels could not be correlated because both levels were either within or below the levels T12 through L3, that is, the segment for physiologic murine hind limb innervation. Thus, a conclusive correlation could only be done in 54% (n = 21) of all functionally tested animals (n = 39) because their skeletal level was within T12 through L3 and the corresponding neurocutaneous level below L3. Of those, we found that in 52.5% (n = 11), the functional result corresponded with the neurocutaneous level, whereas in 47.5% (n = 10), it corresponded with the skeletal level.

### 3. Discussion

The present study shows in a fetal mouse model of naturally occurring MMC that the cutaneous and neural dysraphism coincide consistently and precisely, whereas the skeletal dysraphism differs significantly from the former at the cranial end. In particular, the skeletal lesion is always larger than the corresponding neurocutaneous lesion because of the cranially higher level of the skeletal lesion. Finally, correlation of functional and anatomical levels (where feasible) indicates that the functional level correlates slightly more frequently with the neurocutaneous than with the skeletal dysraphism.

An explanation for the striking morphological coincidence of neural and cutaneous levels as well as for the distinct difference between neurocutaneous and skeletal levels can be drawn from development. Of note, neurulation in this animal model is accomplished by E10.5 [7], whereas fusion of the vertebral arches occurs significantly later and is accomplished by E16.5, as described in this study. If the pathogenic mechanism causing dysraphism hits all involved tissues (notably after separation of neural tissue from the ectodermal plate has occurred, which is a prerequisite for development and fusion of the mesoderm-derived vertebral arches) at the lesion site rather simultaneously than sequentially, which we think is a reasonable assumption, then neurulation is more advanced than vertebral arch closure at the point when fusion processes stop. As a result, the skeletal dysraphism is more extended, as shown here. Moreover, because the neural tube derives from a thickened ectodermal area in the dorsal midline, and thus stems from the same germ layer as the epidermis [8], it is tenable to assume that a dysraphic developmental disorder affects both tissues at the same level. This would explain why neural and cutaneous levels coincide.

The most intriguing aspect of this study is the fact that, in roughly half of the animals amenable to this sort of testing, the neurologic functional level correlated with the more caudally located soft tissue opening and not with the more cranially sited bony defect. It is a plausible explanation that soft tissue directly overlying the spinal cord because of missing dorsal arches may protect the neural tissue. On the other hand, it is unclear why the suggested protective effect is only present in half of the sample studied.

This interpretation is in accord with the nowadays widely accepted concept that soft tissue coverage protects an underlying, in particular, normal, spinal cord from progressive degeneration and loss of function with ongoing pregnancy. In fact, there is an impressive body of experimental and clinical evidence pointing at the fact that normal as well as nonneurulated spinal cord tissue is progressively destroyed in utero if openly exposed to the amniotic cavity [9-15] and, in turn, that timely in utero coverage of exposed spinal cord tissue may salvage function at birth [16-19]. Furthermore, several authors [1,2,15,20] describe patients with MMC with a neural placode that shows a skin defect but is covered with a thin membrane. Consequently, these patients have only moderate or mild, if any, functional deficits.

Interestingly, some findings of this murine study do not exactly relate to the situation found in humans. First of all, the cutaneous MMC defect in humans can be at any level of the spine but usually does not run down to the coccygeal vertebrae, whereas the underlying spinal cord is almost always defective to the end of the conus [21]. Second, from our own (unpublished) clinical experience, levels of the skeletal and skin dysraphism usually differ little, if any. Also, the functional levels are mostly located within the lesion area and do not regularly coincide with the radiologic (skeletal) or

with the anatomical (skin) defect. Similar observations are cited in the literature [13,20-24]. For instance, Hunt et al [13,23] found the sensory level present at birth being the best predictive factor for long-term outcome in terms of mobility, continence, and overall disability rather than radiologic (skeletal), cutaneous, or motor activity level at birth. In contrast, other authors found that the anatomical level obtained by prenatal ultrasound was the best predictive factor rather than radiographic or neuromotor levels found at birth [20,21,24]. Finally, Luthy et al [25] reported that the outcome depended on whether cesarean delivery before onset of labor was performed or not.

In conclusion, this study shows that, in fetal and neonatal mice with genetically determined MMC, the cutaneous and neural dysraphic levels coincide, whereas the skeletal dysraphism is significantly larger rostrally. Importantly, in a subset of animals, we found evidence that naturally occurring skin coverage over the lesion might exert a protective, that is, function sparing effect toward the underlying neural tissue. These functional findings are in agreement with and thus corroborate the rationale for fetal surgery in human patients with MMC.

## Acknowledgment

We thank Professor A. J. Copp at the Institute of Child Health, University College London, London, UK, for his support and critical inputs during the study.

## References

- [1] Hutchins GM, Meuli M, Meuli-Simmen C, et al. Acquired spinal cord injury in human fetuses with myelomeningocele. *Pediatr Pathol Lab Med* 1996;16:701-12.
- [2] Meuli M, Meuli-Simmen C, Hutchins GM, et al. The spinal cord lesion in human fetuses with myelomeningocele: implications for fetal surgery. *J Pediatr Surg* 1997;32(3):448-52.
- [3] Kodama N, Sekiguchi S. The development of spontaneous body movement in prenatal and perinatal mice. *Dev Psychobiol* 1984;17(2): 139-50.
- [4] Suzue T. Movements of mouse fetuses in early stages of neural development studied in vitro. *Neuroscience letters* 1996;218:131-4.
- [5] Stiefel D, Copp AJ, Meuli M. Fetal spina bifida: loss of neural function in utero. *J Neurosurg (3 Suppl Pediatrics)* 2007;106:211-21.
- [6] Zeman W, Craigie EH, Innes JRM. Craigie's neuroanatomy of the rat. New York: Academic Press; 1963.
- [7] Stiefel D, Meuli M. Scanning electron microscopy of fetal murine myelomeningocele reveals growth and development of the spinal cord in early gestation and neural tissue destruction around birth. *J Pediatr Surg* 2007;42:1561-5.
- [8] Copp A, Brook FA, Estibeiro JP, et al. The embryonic development of mammalian neural tube defects. *Prog Neurobiol* 1990;35:363-403.
- [9] Emery JL, Lendon RG. Clinical implications of cord lesions in neurospinal dysraphism. *Dev Med Child Neurol* 1972;14(Suppl 27): 45-51.
- [10] Osaka K, Tanimura T, Hyraima A, et al. Myelomeningocele before birth. *J Neurosurg* 1978;49:711-24.
- [11] Korenromp MJ, Van Gool JD, Bruinse HW. Early fetal leg movements in myelomeningocele. *Lancet* 1986;1:917-8.
- [12] Heffez DS, Aryanpur J, Hutchins GM, et al. The paralysis associated with myelomeningocele: clinical and experimental data implicating a preventable spinal cord injury. *Neurosurgery* 1990;26:987-92.
- [13] Hunt GM. Open spina bifida: outcome for a complete cohort treated unselectively and followed into adulthood. *Dev Med Child Neurol* 1990;32:108-18.
- [14] Shapiro E, Sellar MJ, Lepor H, et al. Altered smooth muscle development and innervation in the lower genitourinary and gastrointestinal tract of the male human fetus with myelomeningocele. *J Urol* 1998;160:1047-53.
- [15] Oya N, Suzuki Y, Tanemura M, et al. Detection of skin over cysts with spina bifida may be useful not only for preventing neurological damage during labor but also for predicting fetal prognosis. *Fetal Diagn Ther* 2000;15:156-9.
- [16] Michejda M. Intrauterine treatment of spina bifida: primate model. *Z Kinderchir* 1984;39:259-61.
- [17] Heffez DS, Aryanpur J, Cuello Rotellini NA, et al. Intrauterine repair of experimental surgically created dysraphism. *Neurosurgery* 1993;32:1005-10.
- [18] Meuli M, Meuli-Simmen C, Yingling CD, et al. In utero surgery rescues neurological function at birth in sheep with spina bifida. *Nature Med* 1995;1(4):342-7.
- [19] Adzick NS, Sutton LN, Crombleholme TM, et al. Successful fetal surgery for spina bifida. *Lancet* 1998;352:1675-6.
- [20] Kollias SS, Goldstein RB, Cogen PH, et al. Prenatally detected myelomeningoceles: sonographic accuracy in estimation of the spinal level. *Radiology* 1992;185:109-12.
- [21] Cochrane DD, Wilson RD, Steinbok P, et al. Prenatal spinal evaluation and functional outcome of patients born with myelomeningocele: information for improved prenatal counselling and outcome prediction. *Fet Diagn Ther* 1996;11:159-68.
- [22] Barson AJ. Spina bifida: the significance of the level and extent of the defect to the morphogenesis. *Dev Med Child Neurol* 1970(12):129-44.
- [23] Hunt G, Lewin W, Gleave J, et al. Predictive factors in open myelomeningocele with special reference to sensory level. *BMJ* 1973; 4:197-201.
- [24] Coniglio SJ, Anderson SM, Ferguson JE. Functional outcome in children with myelomeningocele: correlation with anatomic level on prenatal ultrasound. *Dev Med Child Neurol* 1996;38:675-80.
- [25] Luthy DA, Wardinsky T, Shurtleff DB. Cesarean section before the onset of labor and subsequent motor function in infants with myelomeningocele diagnosed antenatally. *New Engl J Med* 1991; 324:662-6.